Proceedings of the ASME 2021 15th International Conference on Energy Sustainability
ES2021
June 16-18, 2021, Virtual, Online

ES2021-62746

NUMERICAL ASSESSMENT OF PACKING STRUCTURES FOR GAS-PARTICLE TRICKLE FLOW HEAT EXCHANGER FOR APPLICATION IN CSP PLANTS

Markus Reichart
German Aerospace Center - Institute of Solar Research
Stuttgart, Germany

Martina Neises-von Puttkamer
German Aerospace Center - Institute of Solar Research
Stuttgart, Germany

Reiner Buck
German Aerospace Center - Institute of Solar Research
Stuttgart, Germany

Robert Pitz-Paal
German Aerospace Center - Institute of Solar Research
Colone, Germany

ABSTRACT

The centrifugal particle receiver (CentRec), a direct absorbing receiver operating with ceramic particles, demonstrated at the Julich solar power tower under solar conditions technical large-scale feasibility, generating particle outlet temperatures up to 965 °C. To push particle based CSP technology further towards commercial application the high particle temperatures have to be transferred to a working fluid, like air. A gas-particle trickle flow direct contact heat exchanger (TFHX) has been identified with great potential for high efficiency heat transfer. Inspired by chemical trickle flow reactors and previous work in literature focusing on the gas-particle TFHX concept for temperatures up to 500 °C, the approach and its applicability for high temperature heat exchanger shall be developed further in future. In preparation for subsequent research activities, the present work focuses on the preliminary selection of suitable packing structures for the TFHX. Packing assessment criteria are defined and used to assess the particle behavior within a variety of 44 different packing geometries. The analysis was performed using the open source DEM software LIGGHTS-PUBLIC whereas at this early stage of investigation gas presence was neglected. In the analysis process the packing structures are assessed with the previously defined assessment criteria and reduced to one type of a favorable geometry type. In conclusion, the advantageous characteristics of the identified geometry type are discussed. The presented study gives a methodical selection for packing structures and first starting point for further investigating in the field of the gas-particle TFHX whereas in subsequent work the influence of gas flow to the particle dynamic must be investigated by experimental and simulation work.

Keywords: trickle flow reactor, direct contact heat exchanger, particle air heat exchanger, particle trickle flow, packing geometry, packing structure, CSP

NOMENCLATURE

List of symbols

a	m²/m³	specific volumetric surface area
β	m^3/m^3_{void}	hold-up = particle fraction within packing void
d	m	distance, diameter
$\bar{d}_{32}$	m	Sauter diameter
ϵ	-	coefficient of restitution
ϵ_0	m^3_{void}/m^3	void fraction of packing
g	m/s²	gravitational acceleration (9.81)
μ	-	friction coefficient
$\dot{m}$	kg/s	mass flow
ν	-	Poisson's ratio
P	-	overall mixing composition of two quantities
s_{rel}	-	relative linear particle distribution
s_{n}^2	-	mixing quality of two quantities
ρ	kg/m³	density
σ_0^2	-	fully segregated mixture
σ_{id}^2	-	ideal uniform mixture
σ_z^2	-	stochastic uniform mixture
u	m/s	velocity
V	m³	volume
w	m	width
X	-	sample mixing composition
Y	MPa	Young's modulus

Subscripts

A	component A
bar	bar
dyn	dynamic
DC	discrete cell
h	horizontal
i	sample number
min	minimum
n	number of samples
p	particle

pp	particle-particle interaction
pw	particle-wall interaction
pac	packing
R	rolling friction
S	sliding friction
sa	sample, containing component A and B
stat	static
t	terminal
tot	total
v	vertical
y	y-direction

1. INTRODUCTION

Research activities in the field of concentrated solar power (CSP) are often motivated in enhancing competitiveness against other technologies. Current state of the art in CSP tower systems often use molten salt for heat transfer fluid (HTF) and are typically limited to the decomposition temperature of salt in the range of 600 °C. One approach to improve CSP systems is to increase the maximum operation temperature. HTFs based on sintered bauxite particles are limited up to its sintering temperature, starting at 1100 °C [1] providing the possibility to increase process temperatures for CSP tower systems.

A new direct absorbing receiver system has been successfully developed and tested by the DLR institute of solar research. The centrifugal particle receiver (CentRec) demonstrated at the Juelich solar power tower 2.5 MW_{th} under solar conditions obtaining particle outlet temperatures up to 965 °C [2]. To push particle based CSP technology further towards commercial applications heat stored in the particles has to be transferred to a working fluid like air to provide high temperature heat for e.g. industrial processes or electricity generation. To obtain high heat exchanger efficiencies it is aimed to take advantage of the available huge heat transfer area provided by the large number of small particles, used as HTF. A gas-particle trickle flow direct contact heat exchanger (TFHX) has been identified with great potential for high efficiency heat transfer. Due to high parasitic losses in fluidized bed (FB) heat exchangers and poor volumetric power densities in cyclone (CY) heat exchangers, state of the art technologies for gas-particle direct contact heat transfer based on e.g. FB or CY systems are considered inferior to the TFHX for the desired task.

Motivated by the chemical, petrol and cement industry research activities in the field of the gas-particle trickle flow reactors were concentrated especially in the 70ties and 80ies, focusing on the overall behavior and hydrodynamics of the particle flow within varying packing structures with countercurrent air flow [3-5]. Investigations focusing on the influence of particle hydrodynamics, characterized by the particle hold-up, particle distribution and segregation have been conducted using dumped packings by e.g. Pall rings or Raschig rings [4, 5]. Large, Guignon and Saatdjian [6] showed that for irregular packing structures particle segregation occurs and the trickling particles form view thick strains resulting in an uneven particle distribution in the cross-sectional area. Verver and van Swaaij [7], Kiel, Prins and van Swaaij [8] studied the particle hydrodynamics of different regular arranged packing structures, using bars or tubes with circular and squared cross-sectional area and showed superior behavior compared to irregular packing structures. Compared to irregular packings they testified, that trickling particles show in regular stacked packing structures better radial distribution. Furthermore, higher particle volume fraction within void of the packing structures (= particle hold-up, β) and lower pressure drop with countercurrent gas flow was observed. A high particle hold-up in trickle flow reactors used for heat exchanger purposes is preferred since β correlates proportionally with the volume specific particle surface within the packed column a_p participating at the heat transfer. To develop corresponding trickle flow heat exchangers with high power densities it is expected that packing structures capable in providing a high volumetric particle surface are beneficial for gas-particle direct contact heat transfer. Therefore, the understanding of particle hydrodynamics to provide a high particle hold-up must be investigated, a pre-selection of suitable packing structures will be the scope of the present work.

Verver and van Swaaij [7] mention their motivation to rotate the horizontal bars with cross-sectional area by 45 ° along the bar-axis "in order to avoid any accumulation of solids" [9]. Furthermore, based on the information available in the reviewed literature, to date no methodical assessment is known in the determination and selection of bar shapes for regular staged packing structures for trickle flow reactors aiming to provide a high particle hold-up and an even particle distribution. This is investigated in the present work by using Discrete Element Method (DEM) without gas presence, comparing the hold-up and the particle distribution for different geometrical structures. The work is a theoretical preliminary study to provide a methodical selection for packing structures and first starting point in the field of the gas-particle TFHX. In further investigations the influence of gas flow to the particle hydrodynamic and its limits like particle entrainment must be investigated.

2. METHODICAL APPROACH

2.1. Packing geometries

As previously described, literature indicates that regular arranged bar structures have to be favorized for the given task compared to irregular packing structures like dumped Pall or Raschig rings. However, accessible work does not go into detail in describing the motivation for the chosen geometries and dimensions of the regular packing structures.

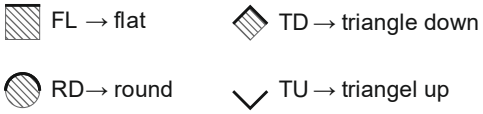

FIG. 1 BASIC OBSTRUCTIVE SURFACES FOR TRICKLING PARTICLES (BOLT) AND POSSIBLE BAR GEOMETRIES (CROSS-HATCHED).

Considering possible bar shapes the resulting surface where the particles trickle over can be reduced to the basic geometries: flat (FL), round (RD), triangle down (TD) like and triangle up (TU) like surfaces, see bolt lines in Fig. 1.

The arrangement of the bar elements is aimed to provide an even particle distribution within the packing and to avoid particle segregation. While passing through the packing structure, an even particle distribution within the TFHX cross sectional area is desired. Therefore, the arrangement of the bar elements will be done in accordance with the procedure proposed by Verver and van Swaaij [7], Kiel, Prins and van Swaaij [8]. Equal distanced horizontal bar layers with a constant number of elements n_{bar} will be used to establish the packing structures. Each second bar layer is rotated by 90° around the y-axis. Furthermore, after two layers n_{bar} is reduced by one bar for the next two layers. Fig. 2 (right) shows e.g. a TD packing structure with n_{bar} = 3. After four layers one packing structure repeats, forming one packing unit (PU).

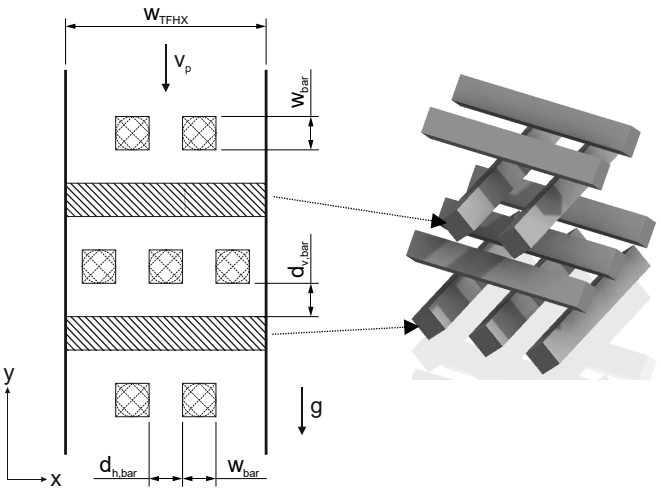

FIG. 2 GENERIC PACKING DIMENSIONING (LEFT) AND EXAMPLE OF PACKING UNIT USING TD BARS (RIGHT)

Fig. 2 (left) illustrates the dimensioning of the packing assembly. The bar width and height are set to be equal w_{bar}. The distance between two bars and two bar layers is described by $d_{\mathrm{h,bar}}$ and $d_{\mathrm{v,bar}}$. The labeling of the different geometry configurations starts with one of the four basic bar shapes, see Fig. 1 followed by the bar width w_{bar} in mm and number of bars per layer n_{bar}. E.g. FL_w04_n4 describes a packing structure generated of flat bar elements with 4 mm width and 4 bars per layers. The minimal distance between the bar elements is limited by the distance where particle arching is expected to occur. Due to Woodcock and Mason [10] the minimum distance must be 10 times the particle diameter to avoid bridging. For approx. 1 mm particles, the minimum bar distance is estimated to 10 mm.

Eleven geometry dimensions providing bar distances in the range of the estimated bridging distance are chosen and marked bolt, see Tab. 1. The table shows $d_{\mathrm{h,bar}}$ for varying geometry configurations with w_{TFHX} = 50 mm.

$$d_{\mathrm{h,bar}} = \frac{w_{\mathrm{TFHX}}}{n_{\mathrm{bar}}} - w_{\mathrm{pac}} \qquad (1)$$

The vertical distance between two layers is set equal to the horizontal distance of the maximum bar number of each bar width available in Tab. 1. For example, $d_{\mathrm{v,bar}}$ of the geometry settings w08_n3 and w08_n2 is equal 9 mm, whereas $d_{\mathrm{v,bar}}$ = 6 mm for w04_n3, w04_n4 and w04_n5.

TAB. 1 DISTANCES BETWEEN BARS IN mm $d_{\mathrm{h,bar}}$ = f(n_{bar},w_{bar})

w_{bar} mm \ n_{bar}	1	2	3	4	5	6
4	46	21	**12.7**	**8.5**	**6**	4.3
6	44	19	**10.7**	**6.5**	4	2.3
8	42	**17**	**8.7**	4.5	2	0.3
10	40	**15**	**6.7**	2.5	0	
12	38	**13**	**4.7**	0.5		
	$d_{\mathrm{h,bar}}$> 20	20 > $d_{\mathrm{h,bar}}$> 10	10 > $d_{\mathrm{h,bar}}$> 0		$d_{\mathrm{h,bar}}$ < 0	

2.2. Assessment criteria for packing structures

For optimized gas-particle heat transfer the assessment criteria for the different geometry settings can be deduced by the defined packing requirements.

- High particle retainment and residence time due to the obstruction exerted by the packing structure, resulting in reduced mean particle falling velocity in y-direction, u_{p}, and increased particle hold-up and thus volumetric particle surface area a_{p} within the TFHX.
- To establish gas flow through the trickling particles, even particle distribution in the TFHX cross sectional area is desired to avoid particle segregation.

The grade of particle retainment within the packing is assessed by the averaged particle velocity in y-direction u_{p}. The overall particle distribution can be expressed using the mixing quality of two components A and B, whereas A can be regarded as the trickling particles and B can be considered as the void fraction, including the packing volume between the trickling particles. The mixing quality s_{n}^2 is calculated by the mean quadratic deviation of empirical variance from n samples X_i for a known overall mixing composition P of the two components [11].

$$s_{\mathrm{n}}^2 = \frac{1}{n}\sum_{i=1}^{n}(X_i - P)^2 \qquad (2)$$

Whereas the sample mixing composition X_i and the overall mixing composition of two quantities P is calculated as follows:

$$P = \sum_{i=1}^{n} X_i = \frac{\sum_{i=1}^{n} V_{\mathrm{A},i}}{\sum_{i=1}^{n} V_{\mathrm{sa},i}} = \sum_{i=1}^{n} \frac{V_{\mathrm{A},i}}{V_{\mathrm{sa},i}} \qquad (3)$$

The calculated mixing quality s_{n}^2 is compared to the inherent limited nature of mixtures, described by fully segregated

mixtures σ_0^2, representing the worst case of particle distribution, regarding the desired task.

$$\sigma_0^2 = P(1-P) \quad (4)$$

An ideal uniform mixture σ_{id}^2 where all components are perfectly equally distanced and distributed is defined as follows.

$$\sigma_{\mathrm{id}}^2 \equiv 0 \quad (5)$$

In practical terms, the best mixing quality achievable with mechanical mixing can be described with the stochastic uniform mixing σ_{z}^2, compare Fig. 3.

$$\sigma_{\mathrm{z}}^2 = \sigma_0^2 \frac{V_{\mathrm{A}}}{V_{\mathrm{sa}}} \quad (6)$$

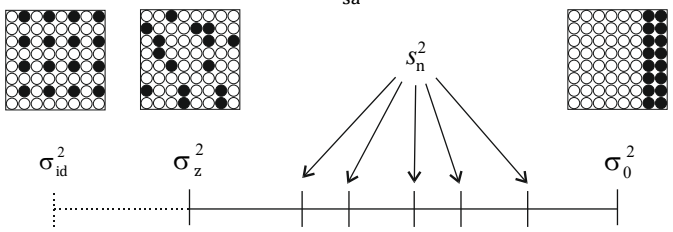

FIG. 3 ASSESSMENT QUALITY OF MIXTURES

2.3. Assessment Procedure

The selected eleven geometrical dimensions, see Tab. 1, and the four bar shapes result in 44 packing geometries to be investigated. Since the scope of this study is to pre-select suitable packing geometries a convenient approach in assessing a variety of packing structures is offered by the simplification of no gas presence within the TFHX. Hence, for simulation approaches no gas volumes have to be generated nor meshed. The trickling particles in the void obstructed by objects were simulated with Discrete Element Method (DEM) using the open source DEM software LIGGHTS-PUBLIC.

At this early stage of investigation, the negligence of air seems feasible since the expected averaged particle sink velocities within the packing are below 0.6 m/s and hence one magnitude below particle terminal velocity u_{t} varying for gas temperatures of 20 °C to 900 °C in the range of 7.9 m/s to 11.3 m/s respectively, using the equation by Kaskas [11] for the drag coefficient of single spheres. Accordingly, for low gas velocities it is expected that the absence of air can be neglected since the exerted drag force of nonmoving air can be estimated by two orders of magnitude lower than the gravitational force of the particles. Experimentally Roes and Van Swaaij [5] confirmed that for low gas flow rates the particle hold-up seems nearly constant, only for higher air flow above the loading point the hold-up starts to increase. However, for further investigations and understanding of gas-particle hydrodynamics gas flow must be taken into account.

Testing in the centrifugal receiver CentRec was conducted using Saint Gobain proppants 16/30 sintered Bauxite [12]. The particle properties are given by Saint-Gobain-Proppants [13] and summarized in Tab. 2.

TAB. 2 PROPERTIES SAINT GOBAIN 16/30 SINTERED BAUXITE [13]

particle size distribution	
diameter (10^{-6} m)	cumulative wt.%
< 595	12
< 841	84
< 1190	4
mean particle diameter	0.98 mm
sphericity	0.9
bulk density	2.04 g/cc

Grobbel [14] investigated the modeling of a solar particle receiver using DEM and therefore performed comprehensive calibration of different particle types and diameters to fit DEM and experimental results at ambient conditions. The parameters required for DEM simulation with Saint Gobain 16/30 sintered bauxite particles used for this work are summarized as follows, provided by Grobbel [14].

$\bar{d}_{32}$ = 1.201 mm Sauter diameter
Y_{p} = 5 MPa Young's modulus
ρ_{p} = 3560 kg/m³ particle density
ν_{p} = 0.3 - Poisson's ratio

coefficient of restitution (COR)

ϵ_{pp} = 0.46 - COR particle-particle contact
ϵ_{pw} = 0.43 - COR particle-wall contact

coefficient of friction (COF)

$\mu_{\mathrm{S,pp}}$ = 0.53 - sliding COF particle-particle contact
$\mu_{\mathrm{S,pw}}$ = 0.31 - sliding COF particle-wall contact
$\mu_{\mathrm{R,pp}}$ = 0.16 - rolling COF particle-particle contact
$\mu_{\mathrm{R,pw}}$ = 0.38 - rolling COF particle-wall contact

The simulations were conducted with two distinct materials, ceramic particles and a packing and wall structure made by steel, with the following parameters.

Y_{w} = 5 MPa Young's modulus
ν_{w} = 0.3 - Poisson's ratio

Using given calibration parameters for the DEM simulations in the present work, the same boundary conditions are used as provided by Grobbel [14].

- Sauter diameter $\bar{d}_{32}$ is used for the representative diameter in DEM simulation
- Particles are assumed to be perfect spheres
- Contact Force Model: tangential history model
- Rolling Friction Model: modified elastic-plastic spring dashpot (EPSD2)

Influence of temperature to the aforementioned parameters is neglected in the present study, since the particle temperature is assumed to be equal to ambient conditions. For further information regarding the calibration procedure and boundary conditions, see Grobbel [14]. There it is mentioned that for the particle-wall rolling friction coefficient $\mu_{\mathrm{R,pw}}$ no intersection

point between calibration experiments and simulations was obtained, this must be considered while interpreting the simulation results.

Typically, the simulation time is set below a fraction of 10 to 30 % of the Rayleigh timestep. It was found that reduction of Young's modulus in DEM simulations to 5 MPa is an acceptable assumption, since particle stiffness showed minor influence to the results, e.g. see [14]. Hence, the simulation time step could be set to 1^{-5} s.

By stacking two packing unit's vertically the particle flow in the DEM simulation can develop in the first PU where the particle mass flow was seeded evenly distributed over the structure. In the second PU the analysis of particles was performed, see Fig. 4. The packing unit is discretized in approximately 1000 discrete cells (DC). For each analyzed time step all particles and its velocity vectors in the PU are assigned to the discrete cells according the position of each particle. Using equations (2) and (3) the particle concentration X_i and mixing quality s_n^2 for the PU can be calculated for each discrete cell, where $V_{sa,i}$ is set equal to $V_{DC,i}$.

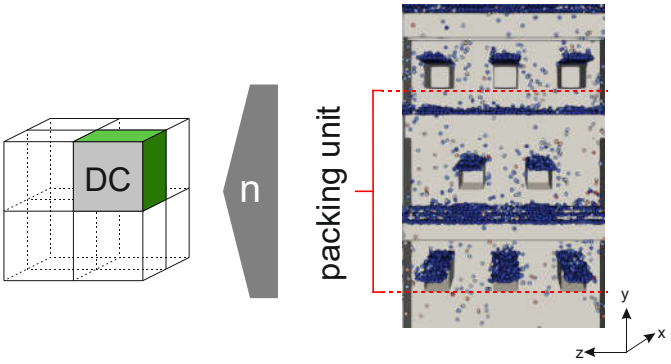

FIG. 4 SCHEME OF DISCRETIZED PU LOCATED BELOW PU FOR DISTRIBUTING THE RANDOMLY SEEDED PARTICLES IN DEM SIMULATION

Fig. 4 (right) shows that packing geometries with bar shapes providing cavities or flat surfaces granules can accumulate in static zones with non-trickling or -moving particles β_{stat}. Whereas, the volume fraction of moving particles in motion and trickling within the packing structure show some minimum dynamic behavior β_{dyn}. In the evaluation procedure the minimum particle velocity $u_{min,dyn}$ is determined for each geometry separating the dynamic particles from the non-moving static particles.

$$\beta_{tot} = \beta_{dyn} + \beta_{stat} \qquad (7)$$

Steady-state within the packing unit is obtained when the seeding mass flow in the model equals the particles flow rate leaving the simulation domain resulting in converging particle total hold-up β_{tot}. The volume fraction of trickling particles within the column β_{dyn} is in the range of 1 % or below and hence can be regarded as diluted gas-particle flow [15]. To assess the simulation results with statistical significance, after reaching steady-state, sensitivity analysis showed that the results of 50 time steps must be averaged for all discrete cells taking into account that for dilute particle flow the positions and distribution of the dynamic particles show some fluctuation.

3. RESULTS AND DISCUSSION

DEM simulations were conducted for the mentioned 44 packing geometries. The gas velocity must be below particle terminal velocity u_t varying from 20 °C to 900 °C in the range of 7.9 m/s to 11.3 m/s respectively. Assuming equal heat capacity flows within the TFHX and u_p to be low the particle mass flow rate is estimated to $\dot{m}_p$ = 18 kg/h.

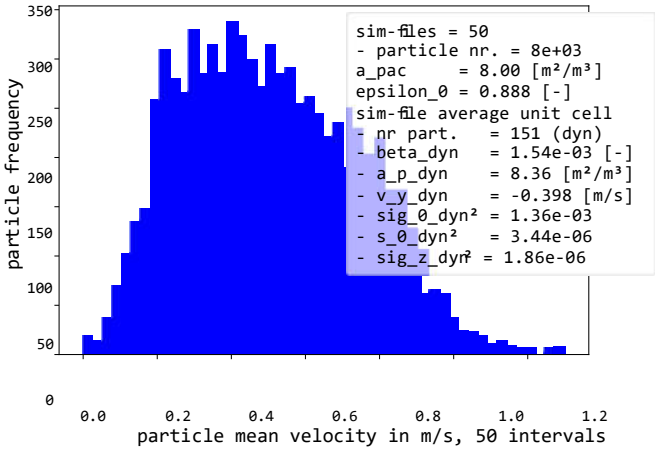

FIG. 5 MEAN-VELOCITY DISTRIBUTION OF ALL PARTICLES IN PACKING UNIT, TD_W04_N4: n_{bar} = 4, w_{bar} = 4 mm, $\dot{m}_p$ = 18 kg/h

For each packing geometry the obstructive character and the mixing quality of the particle flow was calculated. Fig. 5 depicts the particular results for the packing configuration TD_w04_n4. The histogram shows the particle mean velocity distribution and number of occurrences counting the number of particles and assigning the length of each particle mean velocity vector according to the range of the 50 velocity intervals. Since TD shaped bars don't provide the possibility of particle accumulations within the packing structure the dynamic components equal the total components due to the absence of a static particle volume fraction. The averaged velocity in y-direction u_p for all 151 dynamic particles per UC is calculated to -0.398 m/s, affirming the assumption of u_p to be small compared to u_t. The range of u_p and β_{dyn} lies in accordance to the results experimentally investigated by Verver and van Swaaij [7] for low and zero gas flow. Particle distribution can be considered relatively even since $s_{n,dyn}^2$ is located in vicinity close to ${\sigma_z}^2$ compared to ${\sigma_0}^2$. In relative terms the relative linear particle distribution s_{rel} will be defined as follows

$$s_{rel} = \frac{\sqrt{s_n^2} - \sqrt{s_z^2}}{\sqrt{s_0^2} - \sqrt{s_z^2}} \qquad (8)$$

and is for the current case $s_{rel,dyn}$ = 0.9 %.

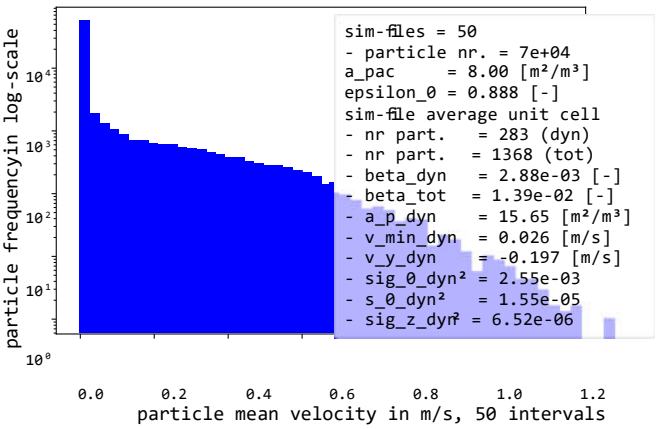

FIG. 6 MEAN-VELOCITY DISTRIBUTION OF ALL PARTICLES IN PACKING UNIT, FL_W04_N4: $n_{bar} = 4$, $w_{bar} = 4$ mm, $\dot{m}_P = 18$ kg/h

Fig. 6 depicts the geometrical configuration FL_w04_n4. Note that the y-axis of the histogram was changed to log-scale since FL shaped bar geometries provide a high grade of particle accumulation. The threshold to distinguish between static or dynamic particles is set to the upper limit of the lowest velocity interval, for the current case $u_{min,dyn} = 0.026$ m/s. A sensitivity analyses after plotting all packing histograms showed 50 velocity intervals suitable to distinguish between static and dynamic particles. In the current example 79.4 % of β_{tot} is assigned to β_{stat}. Changing from TD to FL profile shows an increase in the number of dynamic particles by 87 % to 283 particles. In accordance to equation (9) for the dynamic hold-up stated by e.g. [7, 15]

$$\beta_{dyn} = \frac{\dot{m}_p}{w_{TFHX}^2 \, \epsilon_0 \, \rho_p \, u_p} = \frac{\alpha_{p,dyn} \, d_p}{6 \, \epsilon_0} \qquad (9)$$

u_p reduces by approx. 53 % to ≈ -0.2 m/s. The particle distribution is near to stochastically uniform mixing with $s_{rel,dyn} = 0.2$ %.

Fig. 7 shows for all 44 packing geometries the relative linear particle distribution $s_{rel,dyn}$ in the packing unit with its averaged particle trickling velocity in y-direction, u_p. It shows that the TD and RD packing structures show particle velocities in the range of 0.25 m/s up to 0.6 m/s and particle distribution in the range of approx. 1 % to 6 %. TU profiles show some improvement in particle retainment and distribution compared to TD and RD geometries with 0.19 m/s < u_p < 0.45 m/s and 0.3 % < $s_{rel,dyn}$ < 4 %. Packing structures with FL profiles show the best behavior regarding particle distribution in the range of 0.1 % u_p to 2 % and u_p varying mainly in the range from 0.14 m/s to 0.28 m/s. The reduced velocities for the TU and FL shaped geometries can be explained due to the resting pile of the static particles upon the structures absorbing the kinetic energy of impacting particles, whereas for the TD and RD shaped geometries the particles are mostly deflected in another direction after hitting the structures.

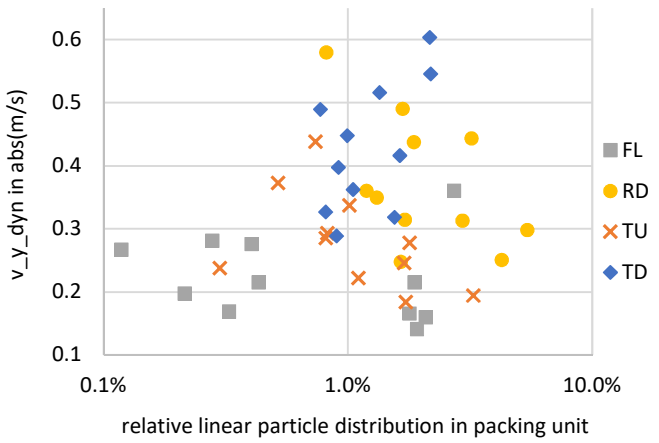

FIG. 7 PARTICLE DISTRIBUTION OF DYNAMIC PARTICLES VS. PARTICLE VELOCITY IN PACKING FOR VARYING GEOMETRIES

Overall the TU and FL shaped profiles show superior behavior regarding particle distribution and retainment compared to TD and RD bars. Whereas FL shaped packing structures show better behavior than the TU profiles. It is assumed that after reaching steady-state the TU shape provide at a certain extent a more stable particle pile for static particles assimilating the form of a TD shaped geometry and approaching its behavior in rather deflecting impacting particles than absorbing impact energy, whereas the particle pile on the FL bars does not offer the same stabilization for the resting particles. It is assumed that the particle piles on FL geometries absorb better the kinetic energy of the impacting trickling particles, resulting in higher reduction of averaged particle velocity in y-direction and hence higher dynamic particle hold-up.

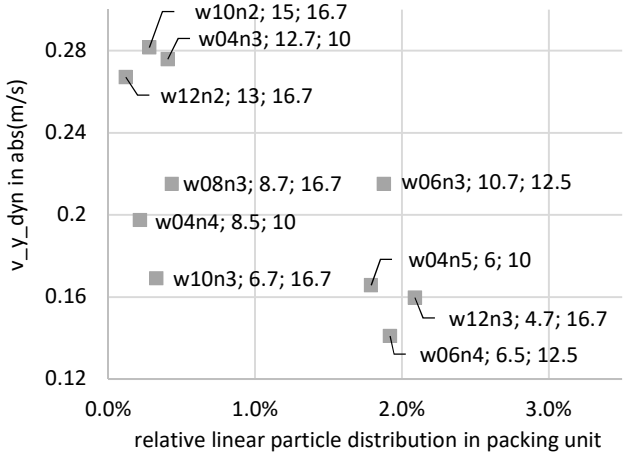

FIG. 8 PARTICLE DISTRIBUTION OF DYNAMIC PARTICLES VS. PARTICLE VELOCITY IN PACKING FOR FL BAR GEOMETRIES WITH ITS CORRESPONDING HORIZONTAL AND FALLING DISTANCES

Fig. 8 depicts a more detailed view of Fig. 7, showing only TL packing geometries. In the diagram the width and number of

bars are displayed and its corresponding horizontal $d_{\mathrm{h,bar}}$ and particle falling distances $w_{\mathrm{bar}} + d_{\mathrm{v,bar}}$. E.g. “w12n2; 13; 16.7” represents the packing geometry with two bars of 12 mm width with $d_{\mathrm{h,bar}}$ = 13 mm and particle falling distance of 16.7 mm. It can be observed that for an increased number of bars and constant w_{bar} the particle retainment increases. Likewise, packing geometries with higher number of w_{bar} and low particle falling distances result in low values for particle velocities in y-direction.

4. CONCLUSION AND OUTLOOK

A methodical selection process was presented to pre-select bar geometries assembled in regular stacked packing structures for trickle flow heat exchanger using DEM simulation with absence of gas influence. It was shown, that all four investigated bar geometries provide a good relative linear particle mixing. Results show that TD and RD profiles are inferior regarding particle retainment and particle distribution compared to the other two bar shapes. FL und TU profile provide a by a factor of two lower particle falling velocity, compared to TD and RD profiles. Relative comparison among the packing structures seems feasible, though the detailed quantitative interpretation of the results must be interpreted carefully since one DEM calibration parameter could not be fitted satisfyingly to the calibration experiments, as described earlier. Therefore also regarding the dimensioning of the geometry setting no final conclusion can made. Either way, for a more detailed view other approaches must be selected where also gas flow must be taken into account. Overall FL profiles show the best particle retainment among the investigated profiles, why for further investigations FL profiles are recommendable.

The presented work provides a starting point for regular arranged profile bars used in particle trickle flow reactors. In future works the particle hydrodynamic under varying air and particle flow rates must by investigated for different packing dimensions also to determine its physical limits like particle entrainment. Subsequently, investigations must be performed at varying temperature conditions to deduce the heat exchanger characteristics. Especially for high temperature application a positive influence of the packing structure is expected since the volume specific surface of the particles and the packing structure are of the same order of magnitude, see Fig. 7 and Fig. 8. High temperature particles e.g. provided by a CSP receiver, entering a TFHX would heat up the packing structure by thermal radiation, causing that the heat transfer in the high temperature zone of the packing would not only take place between air and particles but also between air and packing elements, resulting in increased surface available for heat transfer and hence increased the power density of a gas-particle TFHX.

ACKNOWLEDGEMENTS

This project has received funding from the European Union's Horizon 2020 Research and Innovation Programme under Grant Agreement No 820561.

REFERENCES

[1] Gao, C.-h., Jiang, P., Li, Y., Sun, J.-l., Zhang, J.-j., and Yang, H.-y., 2016, "One step sintering of homogenized bauxite raw material and kinetic study," International Journal of Minerals, Metallurgy, and Materials, 23(10), pp. 1231-1238.

[2] Ebert, M., Amsbeck, L., Rheinländer, J., Schlögl-Knothe, B., Schmitz, S., Sibum, M., Uhlig, R., and Buck, R., 2019, "Operational experience of a centrifugal particle receiver prototype," AIP Conference Proceedings, 2126(1), p. 030018.

[3] Westerterp, K. R., and Kuczynski, M., 1987, "Gas-solid trickle flow hydrodynamics in a packed column," Chemical Engineering Science, 42(7), pp. 1539-1551.

[4] Saatdjian, E., and Large, J. F., 1985, "Heat transfer simulation in a raining packed bed exchanger," Chemical Engineering Science - CHEM ENG SCI, 40, pp. 693-697.

[5] Roes, A. W. M., and Van Swaaij, W. P. M., 1979, "Hydrodynamic behavior of a gas-solid counter-current packed column at trickle flow," The Chemical Engineering Journal, 17, pp. 81–89.

[6] Large, J. F., Guignon, P., and Saatdjian, E., 1983, Multistaging and solids distributor effects in a raining packed bed exchanger.

[7] Verver, A. B., and van Swaaij, W. P. M., 1986, "The hydrodynamic behaviour of gas—solid trickle flow over a regularly stacked packing," Powder Technology, 45(2), pp. 119-132.

[8] Kiel, J. H. A., Prins, W., and van Swaaij, W. P. M., 1992, "Modelling of non-catalytic reactors in a gas-solid trickle flow reactor: Dry, regenerative flue gas desulphurization using a silica-supported copper oxide sorbent," Chemical engineering science, 47(17), pp. 4271-4286.

[9] Verver, A. B., 1984, "The catalytic oxidation of hydrogen sulphide to sulphur in a gas-solid trickle-flow reactor,"Dissertation, University of Twente.

[10] Woodcock, C. R., and Mason, J. S., 1988, Bulk Solids Handling : an Introduction to the Practice and Technology.

[11] Stieß, M., 2009, Partikeltechnologie, Springer, Berlin; Heidelberg.

[12] Ebert, M., Amsbeck, L., Jensch, A., Hertel, J., Rheinländer, J., Trebing, D., Uhlig, R., and Buck, R., 2016, Upscaling, Manufacturing and Test of a Centrifugal Particle Receiver.

[13] Saint-Gobain-Proppants, 2014, "UltraProp/ Sintered Bauxite High Strength Proppants," Summary of Typical Properties, Saint-Gobain.

[14] Grobbel, J., 2019, "Modellierung von solaren Partikelreceivern mit der Diskreten Elemente Methode,"Dissertation, RWTH Aachen.

[15] James, R. M., 2008, "Introduction to particle technology," M. J. Rhodes, ed., Wiley, Chichester, England ; Hoboken, NJ.